ACCOUNTS
of chemical research

Rational Design, Synthesis, Purification, and Activation of Metal−Organic Framework Materials

OMAR K. FARHA AND JOSEPH T. HUPP*

Department of Chemistry and International Institute for Nanotechnology, Northwestern University, 2145 Sheridan Road, Evanston, Illinois 60208

RECEIVED ON APRIL 8, 2010

CONSPECTUS

The emergence of metal−organic frameworks (MOFs) as functional ultrahigh surface area materials is one of the most exciting recent developments in solid-state chemistry. Now constituting thousands of distinct examples, MOFs are an intriguing class of hybrid materials that exist as infinite crystalline lattices with inorganic vertices and molecular-scale organic connectors. Useful properties such as large internal surface areas, ultralow densities, and the availability of uniformly structured cavities and portals of molecular dimensions characterize functional MOFs. Researchers have effectively exploited these unusual properties in applications such as hydrogen and methane storage, chemical separations, and selective chemical catalysis.

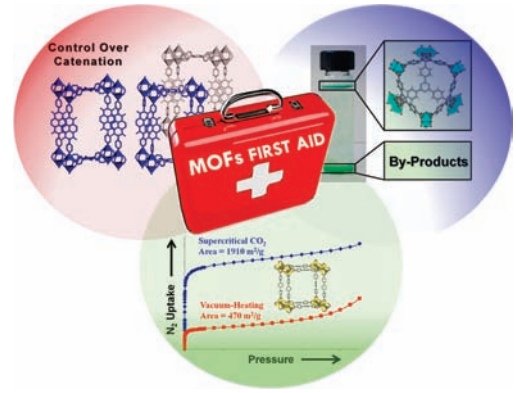

In principle, one of the most attractive features of MOFs is the simplicity of their synthesis. Typically they are obtained via one-pot solvothermal preparations. However, with the simplicity come challenges. In particular, MOF materials, especially more complex ones, can be difficult to obtain in pure form and with the optimal degree of catenation, the interpenetration or interweaving of identical independent networks. Once these two issues are satisfied, the removal of the guest molecules (solvent from synthesis) without damaging the structural integrity of the material is often an additional challenge.

In this Account, we review recent advances in the synthetic design, purification, and activation of metal−organic framework materials. We describe the rational design of a series of organic struts to limit framework catenation and thereby produce large pores. In addition, we demonstrate the rapid separation of desired MOFs from crystalline and amorphous contaminants cogenerated during synthesis based on their different densities. Finally, we discuss the mild and efficient activation of initially solvent-filled pores with supercritical carbon dioxide, yielding usable channels and high internal surface areas.

We expect that the advances in the synthesis, separation, and activation of metal−organic frameworks could lead to MOFs with new structures and functions, better and faster separation and purification of these materials, and processing methods that avoid pore blockage and pore collapse.

Introduction

Metal−organic frameworks (MOFs) are an intriguing class of hybrid materials.[1−3] They exist as infinite crystalline lattices comprising inorganic vertices (metal ions or clusters) and organic struts, connected by coordination bonds of moderate strength (see Figure 1).[4] The most interesting versions of these materials display permanent nanoscale porosity, a feature that can translate into large internal surface areas, ultralow densities, and the availability of uniformly structured cavities and portals of molecular dimensions. Importantly, the crystalline nature of MOF materials allows for unambiguous structure determination by X-ray methods. The resulting knowledge of atomic coordinates makes possible the application of high-

Published on the Web 07/07/2010 www.pubs.acs.org/acr
10.1021/ar1000617

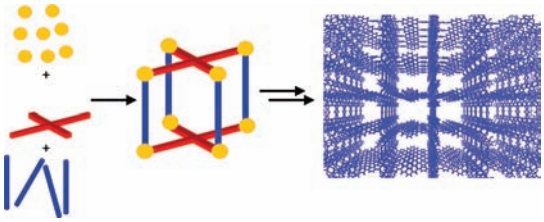

FIGURE 1. General scheme of MOF synthesis.

quality computational modeling of static and dynamic interactions of MOFs with potential sorbents (i.e., predictive or explanative modeling of atomic and molecular isotherms, binding energies, and transport behavior).[5,6] Some of these properties are shared by other porous materials such as zeolites; however, MOFs diverge from zeolites in important ways. Perhaps the most significant difference lies in the element of chemical tunability embedded in the organic components of MOFs; zeolites simply lack organic components as a part of their framework.

Among the many potential applications suggested by the unusual properties of MOFs are gas storage,[7,8] molecular separations,[9–13] chemical catalysis,[14,15] chemical sensing,[16] ion exchange,[17] and drug delivery.[18–20] Indeed, for each of these, multiple proof-of-concept demonstrations have already been reported. For many applications, optimal implementation requires: (a) large pore volumes, (b) phase purity, and (c) retention of porosity upon removal of guest molecules. In many cases, however, these requirements have proven difficult to fully satisfy, thereby preventing the full potential of particular materials from being realized. In our own work, we have increasingly encountered problems along these lines, especially when we have sought to prepare MOFs containing elongated struts or more than one type of strut. As a consequence, we have focused some of our effort on finding broadly applicable solutions to these problems. Our strategies have centered on the following: (a) rational design of organic struts so as to limit framework catenation and thereby produce large pores,[21] (b) rapid separation of desired MOFs from crystalline and amorphous contaminants cogenerated during synthesis,[22] and (c) mild and efficient activation of initially solvent-filled pores. Herein we present an account of our efforts.[23–25]

Controlling Catenation in Metal–Organic Frameworks via Rational Design of the Organic Building Block

As suggested by Scheme 1, MOF structures can consist of either isolated single networks (Scheme 1A) or multiple catenated networks [i.e., two or more identical and independent interwoven (Scheme 1B) or interpenetrated networks (Scheme 1C)]. Internetwork van der Waals interactions provide an energetic incentive for catenation and porous networks may behave as templates for growth of replica networks. Typically, catenation becomes more common as struts are lengthened and initially formed pores become larger. MOF chemists routinely encounter 2- and 3-fold catenation, and examples of considerably higher degrees of catenation are known.[26,27] Catenation can be used to practical advantage if one desires a material with small pore size. Additionally, the interaction of molecular sorbents with catenated structures can give rise to interesting dynamical behavior.[28,29] For example, guest-induced displacement of networks with respect to each other can result in hysteretic sorption, a potentially useful behavior for gas storage or gas-mixture separation.[30]

SCHEME 1. (A) Cartoon Representations of the Noncatenated MOF, (B) the 2-fold Catenated MOF, and (D) the 2D Sheet Formation by the Tetraacid Ligand (red) Pillared by a Dipyridal Strut (blue) and (E, F) Crystallographically Derived *ab*-Plane Looking down the *c*-Channel Using **L9** (E) and **L10** (F)

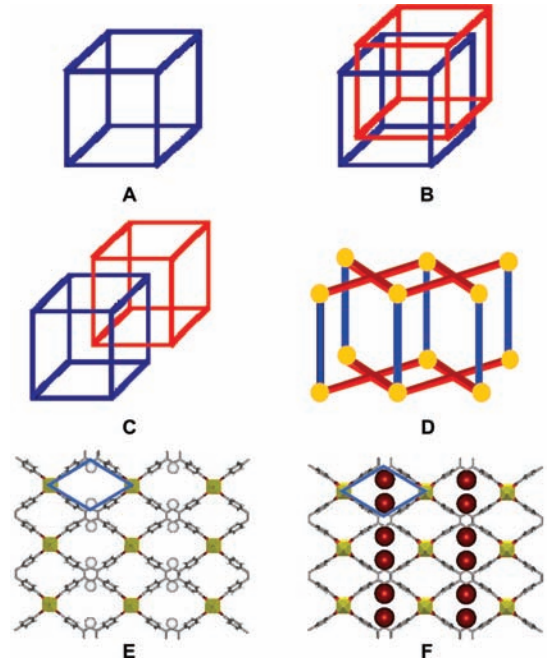

Compared with catenated materials, corresponding noncatenated materials offer larger pores, larger total pore volumes, and lower densities. They also usually offer higher gravimetric surface areas. These properties can be advantageous for applications such as gas storage at high pressure or chemical catalysis involving large substrates.

Ideally one would like to be able to control catenation so as to optimize a given material for a specific application. Several approaches have been explored. In their pioneeering studies of highly symmetrical cubic MOFs, Yaghi and co-workers were able to prepare several pairs of materials of identi-

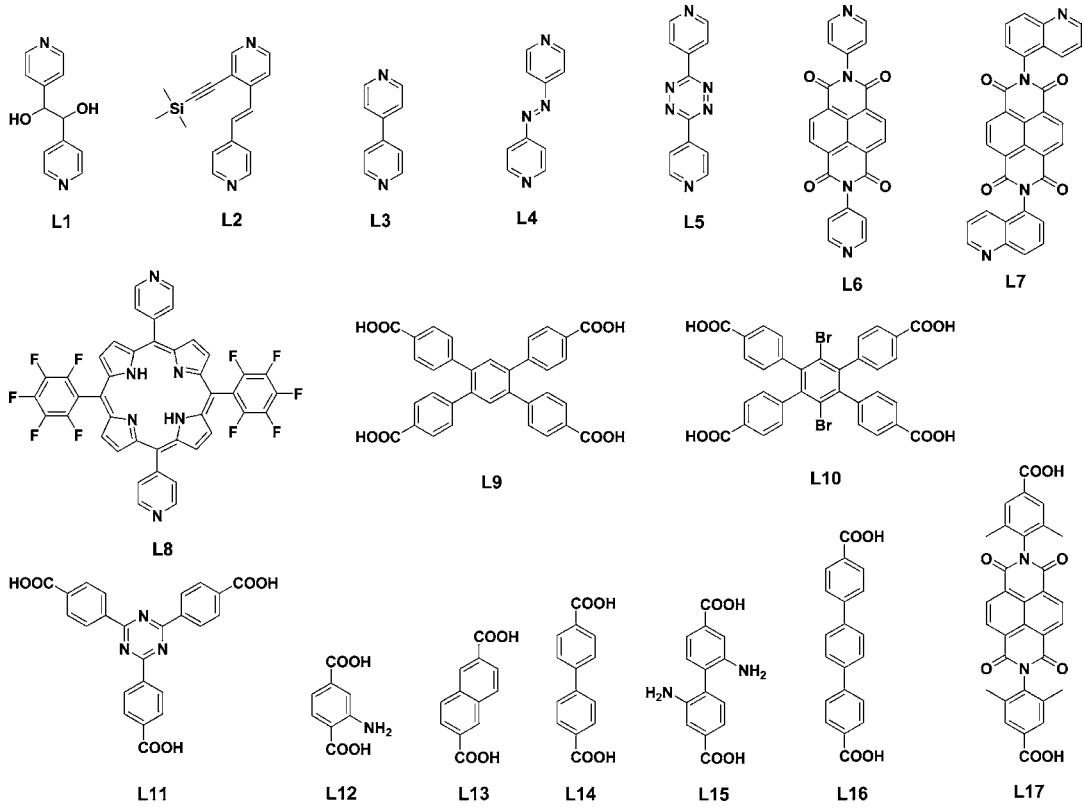

FIGURE 2. Structures of various organic struts employed in the synthesis of MOFs presented in this Account: **L1** = *meso*-α,β-di(4-pyridyl) glucol; **L2** = 3-[(trimethylsilyl)ethynyl]-4-[2-(4-pyridinyl)ethenyl]pyridine; **L3** = 4,4′-dipyridyl; **L4** = 4,4′-azo-dipyridine; **L5** = 1,2,4,5-tetrazine, 3,6-di-(4-pyridinyl); **L6** = *N*,*N*′-di-(4-pyridyl)-1,4,5,8-naphthalenetetracarboxydiimide; **L7** =*N*,*N*′-di-(5-aminoquinoline)-1,4,5,8-naphthalenetetracarboxydiimide; **L8** = (5,15-dipyridyl-10,20-bis(pentafluorophenyl))porphyrin; **L9** = 1,2,4,5-tetrakis(4-carboxyphenyl)benzene; **L10** = 1,4-dibromo-2,3,5,6-tetrakis(4-carboxyphenyl)benzene; **L11** = 4,4′,4″-*s*-triazine-2,4,6-triyltribenzoate; **L12** = 2-aminoterephthalic acid; **L13** = 2,6-naphthalenedicarboxylate; **L14** = 4,4′-biphenyldicarboxylic acid; **L15** = 2,2′-diaminobiphenyl-4,4′-dicarboxylic acid; **L16** = 1,4-di(4-carboxyphenyl)benzene; **L17** = *N*,*N*′-di-(3,5-dimethylcarboxyphenyl)-1,4,5,8-naphthalenetetracarboxydiimide.

cal topology, differing with respect to catenation.[31] Briefly, syntheses run under concentrated conditions tended to yield MOFs characterized by 2-fold catenation, while those run under conditions of very low reactant concentration tended to yield noncatenated structures. By introducing temperature as an additional variable, Zawarotko, Eddaoudi, and co-workers showed that the dilution approach could be extended to an example involving paddlewheel coordination.[32] The need (in most instances) for high dilution to avoid catenation points to a practical limitation of this approach. Only small amounts of material can realistically be synthesized using this method. Both Zhou and co-workers[33] and Lin and co-workers[34] showed that a molecular templating strategy, utilizing oxalic acid, could be used to prevent catenation, although the generality of the approach remains to be tested. Shekhah and co-workers[35] showed that they could obtain a noncatenated MOF by using "liquid-phase epitaxy" on an organic monolayer coated surface and then employing a layer-by-layer growth method. This well-designed work demonstrated that the pillared paddlewheel compound, MOF-508, could be synthesized in noncatenated form. In contrast, standard solvothermal methods invariably generate two interwoven networks.[36,37] However, liquid-phase epitaxy is only relevant for small-scale MOF fabrication, thus limiting the use of this method to surface-related applications. Thus, an alternative, versatile method that can produce substantial quantities of both the catenated and noncatenated versions under similar conditions would be desirable.

We took a different approach to suppressing catenation, focusing on design of the organic component of the MOF (Figure 2). We started by synthesizing a tetracarboxylic acid ligand (1,2,4,5-tetrakis(4-carboxyphenyl)benzene, **L9**, Scheme 2).[38] We envisioned that **L9** would favor the formation of comparatively large cavities and that the ligand's steric demands would inhibit catenation. The combination of **L9** and $Zn(NO_3)_2 \cdot 6H_2O$ under solvothermal conditions produced a noncatenated MOF (**1**) in high yield. Compound **1** (Figure 3) has framework nodes consisting of pairs of zinc ions coordinated by the carboxylates of **L9** in paddlewheel fashion. The strut twists sufficiently to create a true 3D framework, rather than a layered 2D framework. Impor-

SCHEME 2. Synthesis of **L9** and **L10**[a]

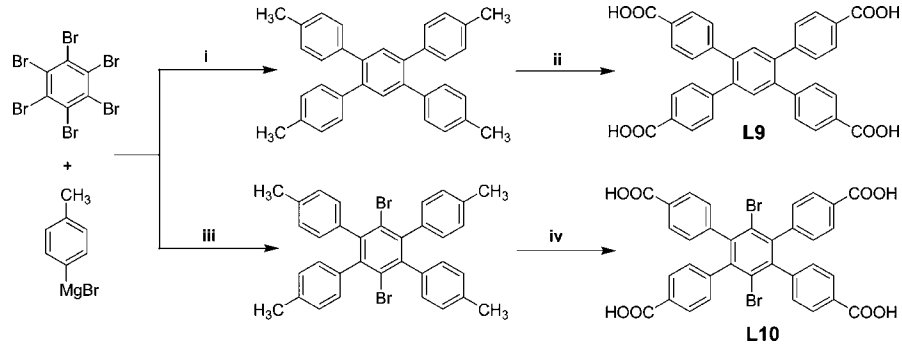

[a] Reagents and conditions: (i) H_2O/HCl; (ii) H_2O/HNO_3; (iii) (a) Br_2, (b) H_2O/HCl; (iv) H_2O/HNO_3.

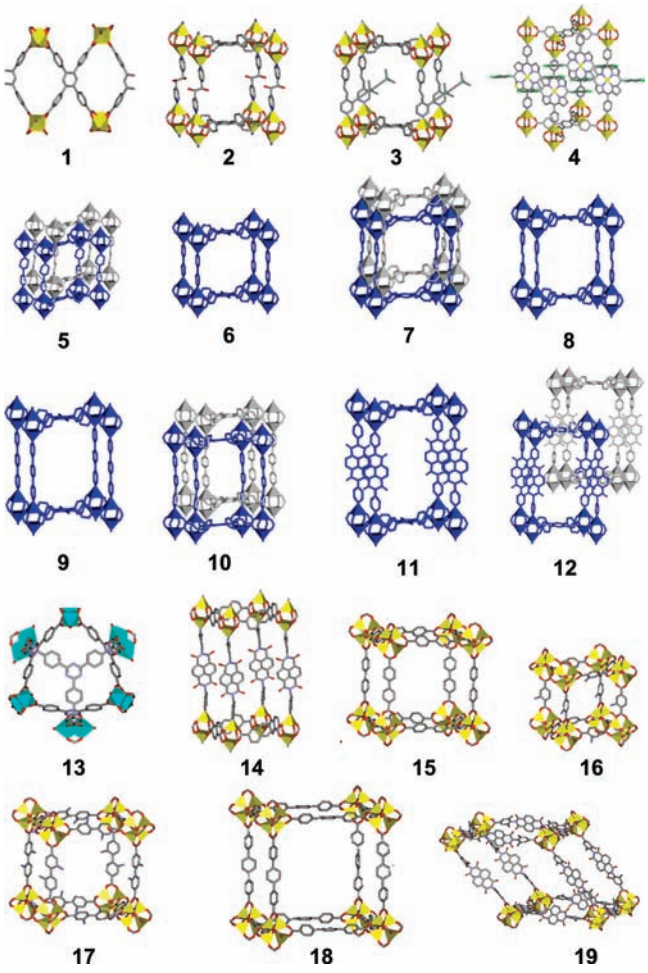

FIGURE 3. Structures of various MOFs employed in this Account. For clarity, interwoven networks and coordinated solvents are omitted. Structures **13**, **14**, and **19** are 2-fold interpenetrated, and the second network is omitted for clarity.

tantly, the axial sites of the $Zn(II)_2$ units are ligated by solvent molecules (omitted in **1** for clarity). (Ligated solvent molecules partially occupy cavities, making catenation difficult. Additionally, because they can be removed and replaced with functional ligands, they provide a convenient means of postsynthetically tailoring cavities.[38])

This finding lead us to employ **L9** in the synthesis of pillared paddlewheel MOFs; we[37] and others[39−41] have previously described pillared paddlewheel materials based upon mixed-ligand Zn(II) coordination of linear dicarboxylates and dipyridyls. These materials are nearly always catenated. Here, we imagined the formation of a 2D sheet within the *xy*-plane defined by **L9**, which could be pillared by a dipyridyl strut as shown in Scheme 1D. We viewed the 2D sheets as *scaffolds* for dipyridyl struts, where tailoring of the dipyridyl component would enable the preparation of MOFs suitable for specific applications.

MOF materials that were made in this fashion produced several examples of noncatenated as well as catenated structures. The noncatenated structures were made via solvothermal syntheses using $Zn(NO_3)_2 \cdot 6H_2O$ and the following combinations: **L8** and **L9**,[42] **L2** and **L9**,[43] and **L1** and **L9**,[44] yielding **4**, **3**, and **2**, respectively. Compound **4** is a rare example of a metalloporphyrin-containing MOF displaying competency for chemical catalysis. Compound **3** was used as a proof-of-principle for selective postsynthesis bifunctional modification via "click" chemistry at the acetylene-containing strut, **L2**. Compound **2** was successfully used to incorporate highly coordinatively unsaturated metal ions that, in principle, could be exploited for gas storage or catalysis.

In contrast, the linear dipyridyl ligand **L6** produced a pillared paddlewheel structure that is 2-fold catenated,[30] where the dipyridyl strut resides directly in the middle of the diamond-shaped cavities formed by two of the **L9** struts as shown in Scheme 1E. The combined results were examined to understand the design weakness that allows only partial, rather than complete, control over catenation. We noticed that in the cases where noncatenated MOFs formed, either a sterically demanding (porphyrin-based (**L8**) or trimethylsilane-protected (**L2**)) or a hydrogen-bonding capable (diol-containing, **L1**) dipyridyl ligand had been used. This led us to conclude

that the sterics of the dipyridyl moiety plays a significant role in the control of catenation.

With the aim of suppressing catenation, **L9** was redesigned by introducing additional steric blockage in the *xy*-plane of the resulting MOF material; see **L10** and Scheme 2.[21] We reasoned that the two large bromine atoms of **L10** would suppress the formation of interpenetrated structures (Scheme 1F). Subsequently, we constructed paddlewheel MOFs using **L10** with the same dipyridyl moieties used to create paddlewheel structures with **L9**. Altogether, four distinct dipyridyl struts (**L3**−**L6**), sterically undemanding but varying in length, were used. A comparison of eight materials, four with strut **L9** (2-fold catenated; **5**, **7**, **10**, and **12**) and four with strut **L10** (noncatenated; **6**, **8**, **9**, and **11**), supported the hypothesis that catenation could be controlled via design of struts. Analysis was done by obtaining a single-crystal X-ray structure of each MOF. The purity of each bulk material was confirmed via powder X-ray diffraction (PXRD).

Thermogravimetric analyses (TGA) of **5**−**12** revealed thermal stability up to ca. 400 °C. As expected, in TGA experiments, the noncatenated compounds **6**, **8**, **9**, and **11** showed greater solvent loss than the 2-fold catenated compounds **5**, **7**, **10**, and **12**. The porosities of **5**−**12** were examined using CO_2 at 273 K; substantially greater surface area was seen for each noncatenated material in comparison to its catenated counterpart.

From these studies, we surmise that the careful design of the organic components of MOFs is as important as the coordination environment in controlling catenation. We are currently investigating other MOF systems to ascertain the extent to which this approach can be generalized.

Density Separation of Different MOF Phases

Metal−organic framework materials (MOFs) are inherently insoluble. This renders impossible the purification of MOFs via the methods usually employed by chemists (distillation, recrystallization, chromatography, sublimation, etc.). Until recently, obtaining pure materials was done by (a) systematically modifying the reaction conditions, which involves many variables such as temperature, solvent composition, reactant concentrations, reaction time, and even reaction vessel size, or (b) manual separation (hand picking) of the desired MOF, which is limited to cases where crystals have different morphology, size, or color. Both methods require time and patience and are somewhat impractical on the large preparatory scale. Therefore, we sought an alternative method for separating MOFs.

Our approach to rapid purification of MOF materials relies upon differences in density between desired and undesired products.[22] In a solvent of appropriate density, one phase of the MOF product mixture floats while the others sink. We found this method to be both straightforward and broadly applicable. In our initial studies, CH_2BrCl was chosen as the starting solvent due to its high density (1.99 g/cm^3) relative to most MOFs. The high solvent density causes all of the solid material to float to the top of the separation apparatus. A second miscible but lighter solvent is added until the appropriate density is reached and the MOF mixture separates into floating and sinking fractions. We found that the method could be readily applied to three commonly encountered scenarios: (a) separation of a desired crystalline MOF from a mixture containing a second compound comprising the same organic-strut and metal-ion building blocks; (b) separation of a mixed-ligand MOF from a second crystalline MOF containing only a single ligand; (c) separation of a noncatenated MOF from an otherwise identical material consisting of catenated networks.

In most cases, a single-crystal X-ray structure of the desired MOF can be obtained even if the bulk material contains impurities. From the single-crystal structure, the anticipated powder X-ray diffraction (PXRD) pattern can be calculated. PXRD measurements can then be used to determine which fraction contains the desired MOF; they also can be used to gauge its purity. One has to keep in mind that the density-separation procedure should be done quickly, before significant solvent exchange with the porous MOFs takes place. Once a solvent of appropriate density is obtained, however, MOF separation occurs very quickly, that is, a few tens of seconds or less.

Example 1: Separation of a Desired Crystalline MOF from a Mixture Containing a Second Compound Comprising the Same Organic-Strut Building Blocks, Metal-Ion Building Blocks, or Both. The synthesis described by Sun et al.[45] of the 2-fold interpenetrated MOF $Cu_3(L11)_2(H_2O)_3$ (**13**) was obtained by reacting $Cu(NO)_2 \cdot 3H_2O$ with **L11** in DMSO at 120 °C. While Sun and co-workers obtained pure **13** (diamond-shaped teal crystals), in our hands the method also sometimes produced a mixture of **13** and a second phase consisting of crystalline green needles that analyzed as having twice the Cu content of **5**. At this point, 20 nominally identical solvothermal synthesis reactions were run. Three yielded the desired MOF in pure form, and five yielded brown amorphous material. The remaining 12 produced a combination of the two crystalline materials in a range of ratios, most of which had the desired product as the minor component (e.g., 15%). The impure compound was purified

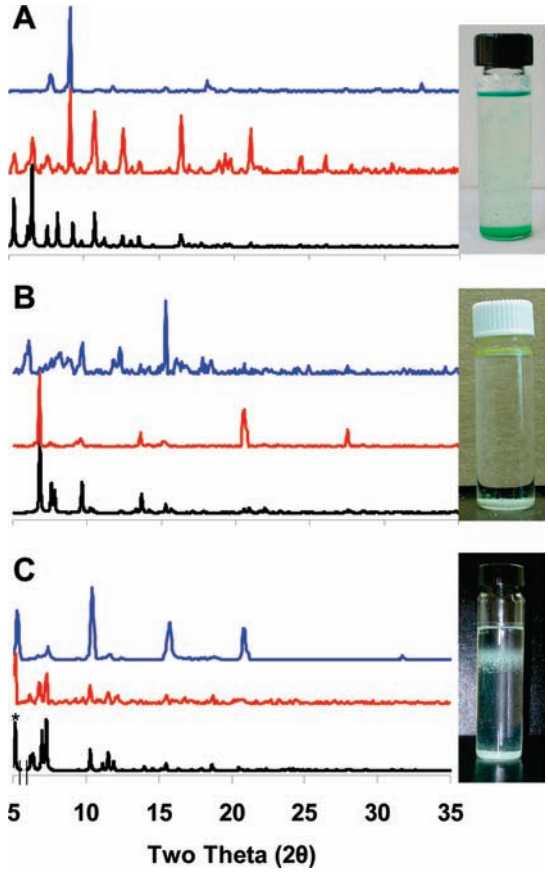

FIGURE 4. PXRD patterns and photos of a vials after separation was achieved for each example: (A) example 1—structure **13** simulation (bottom), **13** after separation (middle), and green needle impurities (top); (B) example 2—structure **14** simulation (bottom), **14** after purification (middle), and white impurities (top); (C) example 3—**15a** simulation (bottom), **15a** after purification (middle), and **15** (top). The peak intensity of the peak marked by ∗ is reduced by 80% in order to elucidate the rest of the spectrum.

by brief sonication, followed by filtration and thorough washing with DMSO. After that, the solid was placed in a separation funnel, followed by addition of 1:5 (v/v) DMSO/CH_2BrCl. Within seconds of the addition, the teal crystals floated to the liquid surface and the green needles sank (Figure 4A). The needles were removed, and the procedure was repeated to ensure the purity of the desired top layer. The purified teal crystals were then collected. A single-crystal X-ray structure, as well as the PXRD pattern of the bulk sample (Figure 4A), confirmed that the desired pure product (**13**) had been isolated. The solvent composition required for the purification was initially ascertained by using pure CH_2BrCl and then adding DMSO until separation was achieved. The density of the solvent should lie between those of the materials to be separated. For verification, the densities of **13** and its impurity were determined via pycnometry and found to be 1.28 and 1.94 g/cm^3, respectively. The density of the solvent mixture was 1.82 g/cm^3.

Example 2: Separation of a mixed-ligand MOF from a Second Crystalline MOF Containing Only a Single Ligand. A doubly interwoven, pillared-paddlewheel MOF, $Zn_2(L13)_2(L7)$ (**14**, yellow crystals), was synthesized by reacting **L13**, **L7**, and $Zn(NO_3)_2 \cdot 6H_2O$ in diethylformamide (DEF).[22] The crude product, however, was contaminated with a white crystalline material. MOF **14** was purified similarly to **13**, but with a solution of 2:5 (v/v) DMF/CH_2BrCl. The desired mixed-ligand compound floated while the contaminant sank. PXRD plots for both fractions are shown in Figure 4B. ^{1}H NMR of an acid-dissolved sample of the contaminant established that it contained **L13** but not **L7**. PXRD data are consistent with formation of an **L13**-based cubic MOF.

Example 3: Separation of a Noncatenated MOF from an Otherwise Identical Material Consisting of Catenated Networks. IRMOF-10 (**15**, a noncatenated material) was synthesized utilizing **L14**, essentially as described by Yaghi et al.,[31] except that DMF replaced DEF as solvent. As is often the case in MOF syntheses, this seemingly minor change had significant consequences: **15** was contaminated with substantial amounts of IRMOF-9 (the 2-fold interwoven analogue of **15**). The mixture was separated using a 4:5:26 (v/v/v) solution of $CH_2Cl_2/CHCl_3/CH_2BrCl$. In this solvent, IRMOF-10 floated, while IRMOF-9 sank (Figure 4C). The PXRD of **15** matched that described by Yaghi and co-workers. To corroborate these results, pure samples of IRMOF-10 and IRMOF-9 were synthesized and then mixed and purified by density separation.

Supercritical Processing of Metal−Organic Framework Materials

MOFs are attractive due to many properties, especially permanent microporosity and large internal surface areas. For most applications, it is necessary to remove guest solvent molecules from the pores of the MOF without the loss of porosity, a process termed "activation". Incomplete or failed activations are typically evidenced by discrepancies between the surface areas that are obtained experimentally after attempted activation and those estimated from computational studies based on single-crystal X-ray structures. Channel collapse upon solvent removal or channel blockage due to partial solvent retention have been invoked to explain these discrepancies. MOFs containing large pores (mesopores) have been found particularly susceptible to incomplete activation.

Traditional activation entails methods for heating the MOF material under vacuum. Unfortunately, in many instances this leads to partial or even full loss of porosity. Yaghi and coworkers were the first to address this problem.[31] They showed

that by exchanging the MOF-incorporated solvent remaining from synthesis for a lower boiling point solvent and then removing the solvent under relatively mild conditions, MOF porosity could often be retained. Nevertheless, in some cases the solvent exchange strategy fails to yield the expected MOF internal surface area. Recently, Ma and co-workers[46] showed that a high internal surface area could be obtained for a representative mesoporous MOF by (a) exchanging the high-boiling-point solvent incorporated in the MOF during the synthesis with benzene and (b) removing the benzene by freeze-drying. The degree of generality of this approach is unknown.

We have reported on an alternative activation protocol entailing processing of solvent-containing MOF materials with liquid and supercritical carbon dioxide (SCD).[23] This method has been previously used for aerogel fabrication,[47,48] where the elimination of surface tension, and therefore capillary forces, prevents the pore collapse that would otherwise occur upon removal of the solvent. In this Account, the four examples presented were chosen due to their instability under most activation conditions.

In all four cases, the MOFs comprise dicarboxylated organic ligands and Zn(II)-containing clusters as nodes. As shown in Figure 5, the SCD approach is capable of very substantially enhancing access to a MOF's internal surface area relative to the following methods: (a) thermally assisted evacuation of the solvent used for synthesis (DMF or DEF) ("conventional activation") and (b) liquid solvent exchange (e.g., DMF ⇔ $CHCl_3$; DEF ⇔ THF) followed by pore evacuation at moderate temperatures (DMF = dimethylformamide; DEF = diethylformamide; THF = tetrahydrofuran).

SCD processing was done with a Tousimis Samdri PVT-30 critical point dryer. The relatively low cost of the dryer (current cost is about $6000) makes this method rather practical. Prior to drying, DMF or DEF solvated MOF samples were soaked in absolute ethanol (EtOH, miscible with CO_2 and compatible with our instrument), replacing the soaking solution every 24 h for 3 days. After soaking, the ethanol-containing samples were placed inside the dryer, and the ethanol was exchanged with $CO_{2(l)}$ over a period of 8 h. During this time the liquid CO_2 was vented under positive pressure for 5 min every 2 h. The rate of venting of $CO_{2(l)}$ was always kept below the rate of filling so as to maintain a full drying chamber. Following venting, the chamber was sealed and the temperature was raised to 40 °C (i.e., above the critical temperature for carbon dioxide) at which time the chamber was slowly vented over the course of 15 h.

Example 1: IRMOF-3, 16. IRMOF-3 (**16**),[31] a noncatenated cubic MOF, was constructed from **L12** and

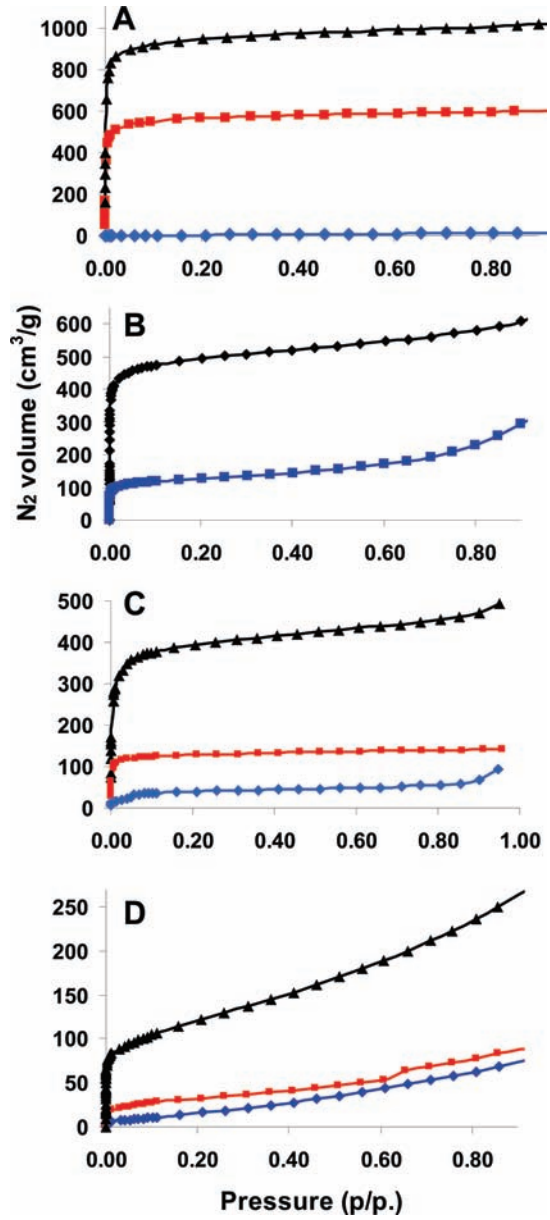

FIGURE 5. N_2 isotherms (77 K) of (A) **16** following SCD activation (top), exchange with $CHCl_3$ followed by evacuation at 25 °C (middle), or conventional activation at 100 °C (bottom), (B) **18** following scd activation (top) or exchange with $CHCl_3$ followed by activation at 25 °C (bottom), (C) **17** following SCD activation (top), exchange with $CHCl_3$ followed by evacuation at 25 °C (middle), or exchange with benzene followed by freeze-dry (bottom), and (D) **19** following ScD activation (top), exchange with THF and evacuation at 25 °C (middle), or conventional activation at 110 °C (bottom).

$Zn(NO_3)_2 \cdot 4H_2O$ in DMF. This material has attracted significant attention because of its susceptibility to postsynthesis covalent modification[49] via the available amine group. This material was activated employing conventional activation, solvent exchange (DMF ⇔ $CHCl_3$), and SCD to yield a negligible surface area, 1800 m^2/g, and 2850 m^2/g, respectively (see Figure 5A.)

Example 2: IRMOF-16, 18. IRMOF-16 (**18**)[31] was synthesized from **L16**, and $Zn(NO_3)_2 \cdot 6H_2O$ in DMF. This material was very hard to handle (moisture sensitive), and to the best of our knowledge, its surface area had not been previously reported. This material showed no porosity when conventional activation was used. Activation of **18** via solvent exchange yielded a N_2-accessible surface area of 470 m^2/g. The surface area was quadrupled via SCD activation (1910 m^2/g; see Figure 5B.)

Example 3: IRMOF-10-NH_2, 17. IRMOF-10-NH_2 (**17**) was synthesized from **L15** and $Zn(NO_3)_2 \cdot 6H_2O$ in DMF. This material has been used to study the effect of amines on CO_2 adsorption. As illustrated in Figure 5C, activation via SCD yielded a surface area of 1525 m^2/g, while chloroform exchange yielded 500 m^2/g.

Example 4: 19.[23] A solvothermal synthesis from a DEF solution of $Zn(NO_3)_2 \cdot 6H_2O$ and **L17** yielded **19**. Compound **19** consists of Zn_4O clusters coordinated by carboxylates in both mono- and bidentate fashion. One water and two DEF molecules also coordinate each node. The coordinated solvents are omitted in Figure 3 for clarity. N_2 adsorption studies (77 K) indicated negligible accessible surface area following conventional thermal activation, while solvent exchange with **19** (THF) yielded a modest Brunauer–Emmet–Teller (BET) surface area of 135 m^2/g. As shown in Figure 5D, the results from SCD activation are striking in comparison, yielding a BET of 400 m^2/g.

From these results, we proposed that the key feature of SCD activation is the elimination of solvent (CO_2) surface tension at temperatures and pressures above the critical point. In addition to (a) preventing collapse of micro- or mesopores and (b) removing channel-blocking solvent molecules, SCD activation appears also to work by preventing undesirable MOF particle agglomeration. Evidence for a role for agglomeration came from (a) the persistence of crystallinity for some MOFs after conventional solvent-exchange and removal, coupled with (b) the inability of these MOFs to adsorb N_2. These observations imply that for some nitrogen-impermeable MOFs, micropores still exist but are largely inaccessible. We have hypothesized that misalignment of micropores at particle/particle boundaries then inhibits access by gas molecules to internal (microporous) surfaces. When re-exposed to liquid solvent, the particles are separated and readily take up solvent molecules (much larger than N_2), as evidenced by subsequent TGA measurements. Thus, the success of SCD activation derives, in part, from its ability to prevent particles from initially agglomerating.

Since our SCD work was published, a report by Tsao and co-workers has appeared.[50] They showed via synchrotron measurements (small-angle X-ray scattering measurements) that MOF particle agglomeration, accompanying conventional activation, leads to elimination of interparticle mesopores, implying external blockage of micropores. Indeed, they conclude that reversible mesopore collapse and accompanying micropore blockage accounts, in part, for lower-than-expected N_2-accessible surface areas in conventionally activated materials.

Concluding Remarks and Prospects

In this Account, we have described our recent work on the rational design of porous MOFs and on the development of efficient methods to purify and activate these materials. We hope that these methods will help advance MOF materials chemistry as follows: (i) Rapid separation of mixtures of MOFs will facilitate MOF discovery and scale-up chemistry. (ii) SCD processing will prevent pore collapse and blockage in delicate MOFs, thereby enabling internal surfaces to be accessed. We anticipate that activation by SCD processing will prove especially useful for MOFs featuring mesopores or comparatively large micropores. (iii) By employment of struts designed to preclude catenation (framework/framework interpenetration), the creation of desired new MOFs featuring unusually large pores and displaying specific functional behavior should prove reasonably straightforward.

We gratefully acknowledge the contributions of several co-workers and colleagues whose names are listed as coauthors in the papers we have cited from our lab. We thank Mr. Brad G. Hauser for providing the data for compound **17**. *We thank DTRA, AFOSR, the U.S. Department of Energy's Office of Science (Grant No. DE-FG02-08ER15967), the Northwestern University Nanoscale Science and Engineering Center, and NU-ICEP for financial support of various aspects of our research on metal–organic framework materials.*

BIOGRAPHICAL INFORMATION

Omar K. Farha is currently a research assistant professor in the Chemistry Department at Northwestern University. He was a National Science Foundation Fellow during his Ph.D. studies. He earned his Ph.D. in Chemistry from the University of California, Los Angeles, under the direction of Prof. M. Frederick Hawthorne. He carried out postdoctoral studies with Prof. Joseph T. Hupp at Northwestern University's Institute for Nanotechnology. His current research focuses on the rational design of metal–organic framework and porous organic polymer materials for catalysis, gas storage, and gas separations.

Joseph T. Hupp holds a Morrison Professorship in the Department of Chemistry at Northwestern University. Prior to joining NU in 1986, he earned a B.S. degree from Houghton College and a Ph.D. from Michigan State. He did postdoctoral work at the University of North Carolina. His current research is focused on photoelectrochemical energy conversion and on the design and synthesis of functional molecular materials.

FOOTNOTES

*E-mail address: j-hupp@northwestern.edu.

REFERENCES

1 O'Keeffe, M.; Peskov, M. A.; Ramsden, S. J.; Yaghi, O. M. The Reticular Chemistry Structure Resource (RCSR) Database of, and Symbols for, Crystal Nets. *Acc. Chem. Res.* **2008**, *41*, 1782–1789.

2 Ferey, G. Hybrid Porous Solids: Past, Present, Future. *Chem. Soc. Rev.* **2009**, *37*, 191–214.

3 Horike, S.; Shimomura, S.; Kitagawa, S. Soft Porous Solids. *Nat. Chem.* **2010**, *1*, 695–704.

4 Tranchemontagne, D. J.; Mendoza-Cortes, J. L.; O'Keeffe, M.; Yaghi, O. M. Secondary Building Units, Nets and Bonding in the Chemistry of Metal-Organic Frameworks. *Chem. Soc. Rev.* **2009**, *38*, 1257–1283.

5 Düren, T.; Bae, Y.-S.; Snurr, R. Q. Using Molecular Simulation to Characterise Metal-Organic Frameworks for Adsorption Applications. *Chem. Soc. Rev.* **2009**, *38*, 1237–1247.

6 Han, S. S.; Mendoza-Cortés, J. L.; Goddard, W. A., III. Recent Advances on Simulation and Theory of Hydrogen Storage in Metal-Organic Frameworks and Covalent Organic Frameworks. *Chem. Soc. Rev.* **2009**, *38*, 1460–1476.

7 Murray, L. J.; Dinca, M.; Long, J. R. Hydrogen Storage in Metal-Organic Frameworks. *Chem. Soc. Rev.* **2009**, *38*, 1294–1314.

8 Hu, Y. H.; Zhang, L. Hydrogen Storage in Metal-Organic Frameworks. *Adv. Mater.* **2010**, *22*, E117–E130.

9 Li, J.-R.; Kuppler, R. J.; Zhou, H.-C. Selective Gas Adsorption and Separation in Metal-Organic Frameworks. *Chem. Soc. Rev.* **2009**, *38*, 1477–1504.

10 Bae, Y.-S.; Farha, O. K.; Spokoyny, A. M.; Mirkin, C. A.; Hupp, J. T.; Snurr, R. Q. Carborane-Based Metal-Organic Frameworks as Highly Selective Sorbents for CO_2 over Methane. *Chem. Commun.* **2008**, 4135–4137.

11 An, J.; Geib, S. J.; Rosi, N. L. Separation: High and Selective CO_2 Uptake in a Cobalt Adeninate Metal−Organic Framework Exhibiting Pyrimidine- and Amino-Decorated Pores. *J. Am. Chem. Soc.* **2010**, *132*, 38–39.

12 Bae, Y.-S.; Farha, O. K.; Hupp, J. T.; Snurr, R. Q. Enhancement of CO_2/N_2 Selectivity in a Metal-Organic Framework by Cavity Modification. *J. Mater. Chem.* **2009**, *19*, 2131–2134.

13 Britt, D.; Furukawa, H.; Wang, B.; Glover, T. G.; Yaghi, O. M. Highly Efficient Separation of Carbon Dioxide by a Metal-Organic Framework Replete with Open Metal Sites. *Proc. Natl. Acad. Sci. U.S.A.* **2009**, *106*, 20637–20640.

14 Lee, J.; Farha, O. K.; Roberts, J.; Scheidt, K. A.; Nguyen, S. T.; Hupp, J. T. Metal-Organic Frameworks Materials as Catalysts. *Chem. Soc. Rev.* **2009**, *38*, 1450–1459.

15 Ma, L.; Abney, C.; Lin, W. Enantioselective Catalysis with Homochiral Metal-Organic Frameworks. *Chem. Soc. Rev.* **2009**, *38*, 1248–1256.

16 Allendorf, M. D.; Bauer, C. A.; Bhakta, R. K.; Houk, R. J. T. Luminescent Metal-Organic Frameworks. *Chem. Soc. Rev.* **2009**, *38*, 1330–1352.

17 Min, K. S.; Suh, M. P. Silver(I)−Polynitrile Network Solids for Anion Exchange: Anion-Induced Transformation of Supramolecular Structure in the Crystalline State. *J. Am. Chem. Soc.* **2000**, *122*, 6834–6840.

18 An, J.; Geib, S. J.; Rosi, N. L. Cation-Triggered Drug Release from a Porous Zinc-Adeninate Metal−Organic Framework. *J. Am. Chem. Soc.* **2009**, *131*, 8376–8377.

19 Horcajada, P.; Serre, C.; Vallet-Regí, M.; Sebban, M.; Taulelle, F.; Férey, G. Metal-Organic Frameworks as Efficient Materials for Drug Delivery. *Angew. Chem., Int. Ed.* **2006**, *118*, 6120–6124.

20 Taylor-Pashow, K. M. L.; Rocca, J. D.; Xie, Z.; Tran, S.; Lin, W. Postsynthetic Modifications of Iron-Carboxylate Nanoscale Metal−Organic Frameworks for Imaging and Drug Delivery. *J. Am. Chem. Soc.* **2009**, *131*, 14261–14263.

21 Farha, O. K.; Malliakas, C. D.; G. Kanatzidis, M. G.; Hupp, J. T. Control over Catenation in Metal−Organic Frameworks via Rational Design of the Organic Building Block. *J. Am. Chem. Soc.* **2010**, *132*, 950–952.

22 Farha, O. K.; Mulfort, K. L.; Thorsness, A. M.; Hupp, J. T. Separating Solids: Purification of Metal−Organic Framework Materials. *J. Am. Chem. Soc.* **2008**, *130*, 8598–8599.

23 Nelson, A. P.; Farha, O. K.; Mulfort, K. L.; Hupp, J. T. Supercritical Processing as a Route to High Internal Surface Areas and Permanent Microporosity in Metal−Organic Framework Materials. *J. Am. Chem. Soc.* **2008**, *131*, 458–460.

24 Bae, Y.-S.; Dubbeldam, D.; Nelson, A. P.; Walton, K. S.; Hupp, J. T.; Snurr, R. Q. Strategies for Characterization of Large-Pore Metal−Organic Frameworks by Combined Experimental and Computational Methods. *Chem. Mater.* **2009**, *21*, 4768–4777.

25 Cooper, A. I.; Rosseinsky, M. J. Metal-Organic Frameworks: Improving Pore Performance. *Nat. Chem.* **2009**, *1*, 26–27.

26 Mulfort, K. L.; Wilson, T. M.; Wasielewski, M. R.; Hupp, J. T. Framework Reduction and Alkali-Metal Doping of a Triply Catenating Metal−Organic Framework Enhances and Then Diminishes H_2 Uptake. *Langmuir* **2008**, *25*, 503–508.

27 Batten, S. R.; Robson, R. Interpenetrating Nets: Ordered, Periodic Entanglement. *Angew. Chem., Int. Ed.* **1998**, *37*, 1460–1494.

28 Kitaura, R.; Akiyama, G.; Seki, K.; Kitagawa, S. Porous Coordination-Polymer Crystals with Gated Channels Specific for Supercritical Gases. *Angew. Chem., Int. Ed.* **2003**, *42*, 428–431.

29 Mulfort, K. L.; Hupp, J. T. Chemical Reduction of Metal−Organic Framework Materials as a Method to Enhance Gas Uptake and Binding. *J. Am. Chem. Soc.* **2007**, *129*, 9604–9605.

30 Mulfort, K. L.; Farha, O. K.; Malliakas, C. D.; Kanatzidis, M. G.; Hupp, J. T. An Interpenetrated Framework Material with Hysteretic CO_2 Uptake. *Chem.—Eur. J.* **2010**, *16*, 276–281.

31 Eddaoudi, M.; Kim, J.; Rosi, N.; Vodak, D.; Wachter, J.; O'Keeffe, M.; Yaghi, O. M. Systematic Design of Pore Size and Functionality in Isoreticular MOFs and Their Application in Methane Storage. *Science* **2002**, *295*, 469–472.

32 Zhang, J.; Wojtas, L.; Larsen, R. W.; Eddaoudi, M.; Zaworotko, M. J. Temperature and Concentration Control over Interpenetration in a Metal−Organic Material. *J. Am. Chem. Soc.* **2009**, *131*, 17040–17041.

33 Ma, S.; Sun, D.; Ambrogio, M.; Fillinger, J. A.; Parkin, S.; Zhou, H.-C. Framework-Catenation Isomerism in Metal−Organic Frameworks and Its Impact on Hydrogen Uptake. *J. Am. Chem. Soc.* **2007**, *129*, 1858–1859.

34 Ma, L.; Lin, W. Chirality-Controlled and Solvent-Templated Catenation Isomerism in Metal−Organic Frameworks. *J. Am. Chem. Soc.* **2008**, *130*, 13834–13835.

35 Shekhah, O.; Wang, H.; Paradinas, M.; Ocal, C.; Schupbach, B.; Terfort, A.; Zacher, D.; Fischer, R. A.; Woll, C. Controlling Interpenetration in Metal-Organic Frameworks by Liquid-Phase Epitaxy. *Nat. Mater.* **2009**, *8*, 481–484.

36 Chen, B.; Liang, C.; Jun, Y.; Contreras, D. S.; Clancy, Y. L.; Lobkovsky, E. B.; Yaghi, O. M.; Dai, S. A Microporous Metal-Organic Framework for Gas-Chromatographic Separation of Alkanes. *Angew. Chem., Int. Ed.* **2006**, *45*, 1390–1393.

37 Ma, B.-Q.; Mulfort, K. L.; Hupp, J. T. Microporous Pillared Paddle-Wheel Frameworks Based on Mixed-Ligand Coordination of Zinc Ions. *Inorg. Chem.* **2005**, *44*, 4912–4914.

38 Farha, O. K.; Mulfort, K. L.; Hupp, J. T. An Example of Node-Based Postassembly Elaboration of a Hydrogen-Sorbing, Metal−Organic Framework Material. *Inorg. Chem.* **2008**, *47*, 10223–10225.

39 Sakamoto, H.; Kitaura, R.; Matsuda, R.; Kitagawa, S.; Kubota, Y.; Takata, M. Systematic Construction of Porous Coordination Pillared-Layer Structures and Their Sorption Properties. *Chem. Lett.* **2010**, *39*, 218–219.

40 Seo, J.; Matsuda, R.; Sakamoto, H.; Bonneau, C.; Kitagawa, S. A Pillared-Layer Coordination Polymer with a Rotatable Pillar Acting as a Molecular Gate for Guest Molecules. *J. Am. Chem. Soc.* **2009**, *131*, 12792–12800.

41 Lee, J. Y.; Olson, D. H.; Pan, L.; Emge, T. J.; Li, J. $[M(bdc)(ted)_{0.5}] \cdot 2DMF \cdot 0.2H_2O$ (M = Zn, Cu): Microporous Metal Organic Frameworks with High Gas Sorption and Separation Capacity. *Adv. Funct. Mater.* **2007**, *17*, 1255–1262.

42 Shultz, A. M.; Farha, O. K.; Hupp, J. T.; Nguyen, S. T. A Catalytically Active, Permanently Microporous MOF with Metalloporphyrin Struts. *J. Am. Chem. Soc.* **2009**, *131*, 4204–4205.

43 Gadzikwa, T.; Farha, O. K.; Malliakas, C. D.; Kanatzidis, M. G.; Hupp, J. T.; Nguyen, S. T. Selective Bifunctional Modification of a Non-catenated Metal−Organic Framework Material via "Click" Chemistry. *J. Am. Chem. Soc.* **2009**, *131*, 13613–13615.

44 Mulfort, K. L.; Farha, O. K.; Stern, C. L.; Sarjeant, A. A.; Hupp, J. T. Post-Synthesis Alkoxide Formation Within Metal-Organic Framework Materials: A Strategy for Incorporating Highly Coordinatively Unsaturated Metal Ions. *J. Am. Chem. Soc.* **2009**, *131*, 3866–3868.

45 Sun, D.; Ma, S.; Ke, Y.; Collins, D. J.; Zhou, H. An Interweaving MOF with High Hydrogen Uptake. *J. Am. Chem. Soc.* **2006**, *128*, 3896–3897.

46 Ma, L.; Jin, A.; Xie, Z.; Lin, W. Freeze Drying Significantly Increases Permanent Porosity and Hydrogen Uptake in 4,4-Connected Metal-Organic Frameworks. *Angew. Chem., Int. Ed.* **2009**, *48*, 9905–9908.

47 Cooper, A. I. Polymer Synthesis and Processing Using Supercritical Carbon Dioxide. *J. Mater. Chem.* **2000**, *10*, 207–234.

48 Lubguban, J. A.; Gangopadhyay, S.; Lahlouh, B.; Rajagopalan, T.; Biswas, N.; Sun, J.; Huang, D. H.; Simon, S. L.; Mallikarjunan, A.; Kim, H.-C.; Hedstrom, J.; Volksen, W.; Miller, R. D.; Toney, M. F. Supercritical CO_2 Extraction of Porogen Phase: An Alternative Route to Nanoporous Dielectrics. *J. Mater. Res.* **2004**, *19*, 3224–3233.

49 Wang, Z.; Cohen, S. M. Postsynthetic Modification of Metal-Organic Frameworks. *Chem. Soc. Rev.* **2009**, *38*, 1315–1329.

50 Tsao, C. S.; Chen, C. Y.; Chung, T. Y.; Su, C. J.; Su, C. H.; Chen, H. L.; Jeng, U. S.; Yu, M. S.; Liao, P. Y.; Lin, K. F.; Tzeng, Y. R. *J. Phys. Chem. C* **2010**, *114*, 7014–7020.